Ahmed GAGA[1,*], Hamid OUANAN[2], Youness MEHDAOUI[1], Benachir EL HADADI[1]

J. Electrical Systems 18-2 (2022): 288-303

Regular paper

low cost PID controller implementation of SEPIC Converter using 8-bits Microcontroller Target for Photovoltaic Applications

Power converters are widely used in renewable energy conversion systems such as photovoltaics. Their main role is to adapt the output voltage to a desired voltage shape. SEPIC is a DC/DC converter that has several advantages over other conventional structures in the same family. It is classified as a conversion structure with complex fourth-order topologies. A multi-physics model under MATLAB/Simulink is used to analyze the time behavior and design the appropriate controller. After system dimensioning, a linear control technique is adopted to generate the control law. The selected controller is PID. After sizing, modeling and simulation of the converter/regulator system, disturbances such as input voltage and load variations will be applied to verify the complete system robustness. Then, the digital PID control algorithm will be implemented on an embedded platform around an 8-bit microcontroller, the PIC18F4550. The controller parameters will be identified experimentally in the overall closed loop system. The results show the reliability of our system in terms of dynamics, stability, and accuracy. The main contribution to this work is the optimization of the PID controller for an 8-bit microcontroller architecture and the application of a SEPIC converter. In addition, we have proposed an online identification method using three potentiometers

.

Keywords: SEPIC Converter, PID controller, Microcontroller, PIC18F4550, DC-DC power converters, Photovoltaic Applications.

1. Introduction

Renewable energies (RE) are energy sources that are naturally renewed fast enough to be considered inexhaustible on a human scale[1]. They derive from cyclical, constant, or random natural phenomena induced by; the Sun for the heat and light that it generates, the wind for the kinetic energy that it produces, or hydraulic energy due to ocean currents[2]. Today, power electronics converters play a vital role in harnessing the energy produced and controlling systems in a wide range of applications, from the smallest, such as power harvesting and integrated devices, to the largest, such as electrical machine control, power generation and transmission[3]. DC-DC power converters are widely used in renewable energy conversion systems, particularly photovoltaics[4]. They are used to adapt the input voltage of a system to the desired output voltage. They are found in MPPT solar regulators[5], photovoltaic inverters, and battery management systems (BMS)[6].

Power converters use electronic components based on semiconductor switches, usually Bipolar, MOSFET or IGBT technology. These transistors operate at different power and

* Corresponding author: Ahmed GAGA, E-mail: gaga.ahmad@gmail.com
[1]Laboratory of Physics and Engineering Sciences, Research team in Embedded Systems Engineering, Automation, Signal, Telecommunications and Smart Materials, Department of Physics, USMS University, BeniMellal 23030, Morocco.
[2]Information Processing & Decision Support Laboratory (TIAD),National School of Applied Sciences,Sultan MoulaySlimane University,BeniMellal, Morocco

frequency levels, ranging from low mains frequencies to high frequencies. In order to optimally take into account the different requirements of various applications, power

converters are classified according to several characteristics[7]. These include isolated or un-isolated converters, powered by current or voltage, and switched either hard-switched or soft-switched. In the literature, there are four different types of conversion between two initial forms of energy (AC-DC, DC-AC, DC-DC and AC-AC)[8][9]. The switch from one form to another depends strongly on the application. For example, domestic grid-connected devices require an AC-DC converter in their energy processing systems, such as televisions. In addition, the integration of renewable energy sources into the grid requires the use of inverters or so-called DC/AC converters to produce a constant or variable alternating voltage output[10][11]. Still, many battery-powered devices use DC-DC converters to provide the DC voltage required by the various internal components. In addition, as mentioned above, DC-DC converters are used to optimize the energy produced by renewable energy sources such as photovoltaic panels and wind turbines[12]. In order to change the voltage or frequency of an AC power source, AC/AC converters are required (e.g. a dimmer switch and a mains frequency changer). Power converters are non-linear systems with a variable and complex structure[13]. Therefore, their performance does not only depend on the design of the hardware part, but it is highly dependent on the adopted control law. For this reason, it is important to understand some basic principles related to power converter control. In the literature, the Average State Space model is used to model and analyze the behavior of DC-DC converters in order to design appropriate controllers[14]. There are three classes of control depending on the choice of the control input.

- PWM-BasedLinear Control
- Control WithoutModulator
- Control With Embedded Modulator

The Pulse With Modulation (PWM) based linear control class presents the most widely used control structure for controlling linear systems, including power converters. In this case, the controller must track the average value of the converter output, which can be either a value of current, voltage, torque, power, etc. Therefore, it generates an average control input (t). This control signal can not be directly operated by the converter. It is synthesized by a modulation stage. Therefore, the controller generates a duty cycle to control the average output value. To design this class of controller, the average model is normally adopted while neglecting the modulator effect[15]. The advantage of using a modulator is that it sets the switching frequency of the converter and produces a well-defined spectrum. Therefore, several control objectives can be met by including the modulator in the control loop. The PWM control technique uses linear controllers such as proportional integral (PI), or proportional integral derivative (PID) or non-linear controllers such as sliding mode, fuzzy logic,etc[16].

In this work, we will present the modeling and dimensioning of a non-isolated DC/DC converter of the SEPIC type in continuous conduction mode (CCM). The converter operates in an environment exposed to different disturbances sources such as variable input voltage or load. This causes a variation in the DC-DC converter operating point. The state-space representation or transfer function is established in the MATLAB/Simulink environment. In addition, Bode and pole diagrams have been drawn for the transfer function of the converter. To regulate the output voltage, a PID regulator will be adopted. Then, a physical simulation will be performed under Proteus ISIS to verify the correct operation of our design using real components. The PID controller will be fully implemented in an 8-bit microcontroller PIC18F4550. It performs two main tasks. The first

one is to execute the algorithm of the digital PID regulator to generate the control law (t). The second one is to transform this control variable into a real PWM output that can be understood by the SEPIC converter using the internal Compare, Capture, PWM (CCP) module of the microcontroller.

SEPIC modeling and sizing

1.1 Electrical Model

The SEPIC (Single Ended Primary Inductor Converter) is a DC-DC converter type that provides a DC output voltage greater than, less than or equal to the input voltage [17]. The output voltage of this converter type is controlled by a PWM signal with a variable duty cycle. The control signal directly drives the power switch used in this converter, which is usually a MOSFET. The hardware structure of the SEPIC converter is shown in Fig. 1. It is similar to the BUCK-BOOST converter, but has the advantage of having a non-inverted output.

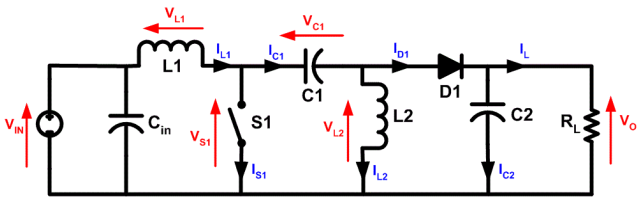

Figure 1: The hardware structure of the SEPIC converter

There are two operating modes of the SEPIC converter, depending directly on the shape of the current IL1 flowing through the input inductor L1. The mode is called continuous conduction mode if the current flowing through inductance L1 never turns off (CCM). In some cases, the amount of energy required by the load is small enough to be transferred in a time shorter than a switching period. In this case, the current flowing through the inductance becomes zero for part of the period, the so-called discontinuous conduction mode (DCM). The SEPIC converter operation study is carried out in two operating phases depending on the conduction state of switch $S1$.

1.2 Convertersizing

Fig. 2 shows the active state of switch S1 (saturated transistor). An input voltage VIN is applied to the input inductor L1 terminal. The current flowing through this inductor will increase linearly, thus storing energy in L1. At the same time, the energy in capacitor C1 passes through inductance L2 and the energy in capacitor C2 passes through charge RL. The output voltage VO is held constant by capacitor C2.

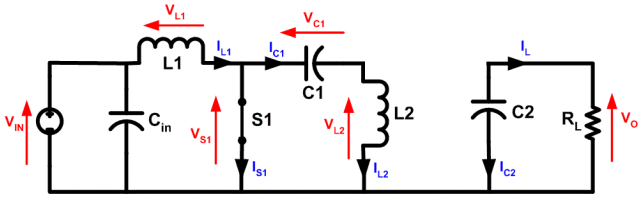

Figure 2: SEPIC Converter ON state

Fig. 3 shows the second operating state of the SEPIC converter, when switch S1 is open (transistor blocked). This state implies that diode D1 is forward biased. Therefore, it is conducted. It allows the current ID1 to flow. Then, the energy stored in the inductor L1 is returned to the capacitor C1 and the stored energy in the inductor L2 is transferred to C2.

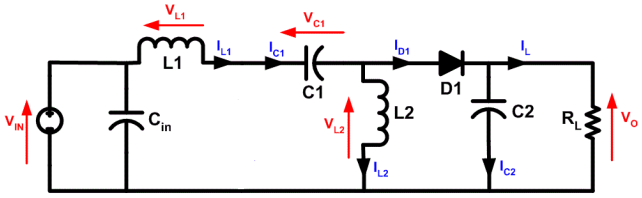

Figure 3: SEPIC Converter OFF state

A PWM signal with a variable duty cycle is used in order to be able to vary the output voltage according to the applied set point in order to have a constant output voltage. The inductance values are mainly determined by the accepted ripple current ΔL. In general, a 40% ripple is allowed[14]. The ripple current flows through inductances of values equal to L1 and L2. C1 is a coupling capacitor inserted at the input to pass the effective current. The capacitor C2 at the output of the SEPIC converter is used to filter the output voltage and keep it constant. The S1 Transistor must be able to support the sum of the two input and output voltages, and to be crossed by a peak current equal to the sum of the peak currents of each inductor. The diode D1 has the same parameters as the transistor S1. It must support a maximal output current. In addition, it must support a reverse voltage equal to the voltage supported by the transistor S1. The TABLE I summarizes all the mathematical expressions governing the parameters that are included in the sizing phase.

TABLE I SEPIC Parameters expressions

Components	Symbol	Expression
Duty Cycle	d	$\frac{V_S + V_D}{V_e + V_S + V_D}$
Ripple Current	ΔI_L	$= I_e \times 40\%$ $= I_s \frac{V_s}{V_e min} \times 40\%$
Inductor 1	L_1	$\frac{V_e min}{\Delta I_L \times f} D_{max}$
Inductor 2	L_2	$\frac{V_e min}{\Delta I_L \times f} D_{max}$
Input Capacitor	C_1	$\frac{I_S \times D_{max}}{\Delta V_{c1} \times f}$
Output Capacitor	C_2	$\frac{I_S \times D_{max}}{\Delta V_{c2} \times f \times 0.5}$

1.3 Sizing results

Based on the analytical expressions given by the equations in TABLE I. The sizing results of the different components of our SEPIC converter are obtained. TABLE II shows the parameter symbol, the analytical value after calculation of the associated expression and the practical value to be used in the real system.

TABLE II SEPIC Parameters values

Parameters	Analytical values	Practical values
L_1	37.085e^{-06} H	40 µH
L_2	37.085e^{-06} H	40 µH
C_1	280.22e^{-06} F	470 µF
C_2	98.077e^{-06} F	100µF
f	50 KHz	50 KHz
d	0.7356	74%
R_L	7.5Ω	10Ω
V_D	0.7 v	0.7 v

PID controller design

1.4 SEPIC converter Model

The main objective of controlling the SEPIC converter in a closed loop is to obtain robust behavior of the output voltage, and to maintain it constant and precise regardless of external disturbances that influence the normal operation of the system. The block diagram of a closed-loop system is shown in **Erreur ! Source du renvoi introuvable.**.

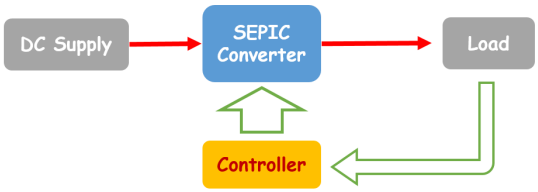

Figure 4: Closed-loop system synoptic diagram

The SEPIC converter is controlled in voltage mode. The PWM modulator is configured with an independent time base. The output voltage is measured by a voltage sensor and sent to the microcontroller. This value is subtracted from the voltage reference in the software part to calculate numerically the voltage error.

This error is then introduced into a control algorithm that produces a duty cycle value based on the current error, the previous error, and the control history respectively. The control algorithm output is also latched to the minimum and maximum duty cycle values for hardware protection. The control algorithm in voltage mode must be executed at a fast rate in order to achieve fast system dynamics. Among the linear control techniques is PID, also called PID corrector (proportional, integral, derivative). It is a control system for improving the performance of a closed-loop control of a given system[18]. It is the most widely used controller in the industry where its correction qualities apply to multiple physical quantities. A PID controller is a calculation algorithm that delivers a control signal based on the difference between the set point and the measurement. It acts in three ways: a proportional action where the error is multiplied by a gain G, followed by an integral action where the error is integrated and divided by a gain $T_i$and finally, a derivative action where the error is derived and multiplied by a gain T_d.

In order to combine these three effects (P, I, and D), we distinguish several possible configurations, which are; serial, parallel, or mixed. In this work, we adopt a parallel PID structure that acts on the error. The equation used to describe the parallel PID controller is

translated into the feedback loop Eq (1). This form is the simplest, sometimes called the parallel equation, because each action (P, I, and D) occurs in separate terms of the equation, the combined effect being a simple sum. The control signal at the output of the PID controller is given by:

$$u(t) = K_p\, \mathrm{e(t)} + K_i \int e(t)dt + K_d \frac{de(t)}{dt} \quad (1)$$

With the control error express as shown in the equation (2).

$$e(t) = Y_{ref} - Y(t) \quad (2)$$

Where (t) is the output measurement, $Y_{ref}$is the reference variable which is often referred to as the set point, and (t) is the control signal generated at the controller output. The control signal is therefore the sum of the following three terms; a proportional term to the error (P), a term proportional to the integral of the error (I) and a term (D) which is proportional to the derivative of the error. The controller parameters are the proportional gain T_p, the time integral T_i, and the derivative time T_d.

1.5 Controller design

In this part, we will show how to design a PID controller for the DC/DC converter SEPIC type presented and dimensioned previously. This power electronics system (SEPIC) will be modeled and simulated in the Simulink environment using SimScape Electrical multi-physics components. Many power electronics systems cannot be linearized because they are variable-structured systems and use high-frequency switching components (transistors in this case), such as the present SEPIC DC/DC converter that incorporates a pulse-width modulator (PWM). However, most PID tuning tools and techniques design PID gains based on a linearized model. To obtain such a model for a system that cannot be linearized, we are faced with two possibilities; either to estimate the parameters of the linear system model using the System Identification Toolbox software, or to estimate the frequency response of the system over a range of frequencies. The complete model including the SEPIC converter plus the PID control chain is given in Figure 5

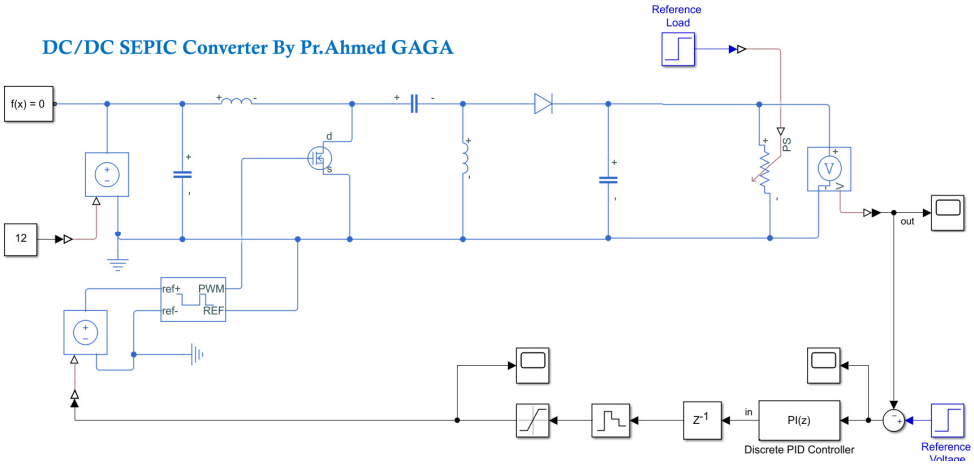

Figure 5: PID Controlled SEPIC converter SIMULINK Model

In this model, a MOSFET controlled by a pulse width modulated (PWM) signal is used to switch the transistor. The output voltage V_{out} must follow the reference value V_{ref}. A digital PID controller takes the voltage error (V_{out} - V_{ref}) at the input and adjusts the PWM duty

cycle at the output according to this error. To design the PID controller, we first need to determine the steady state operating point at which we want the converter to operate. In this work, we will use an operating point estimated from a simulation snapshot. The principle is to specify the initial conditions of the model near an expected steady state point, and simulate the model until it reaches a steady state. One can then create a linear operating model based on the signals and equilibrium states. Afterwards, the model is initialized with the inputs and states of the selected operating point. Before setting the parameters of the PID control block, the structure of the controller must first be specified. Including the type, shape, time domain, initial conditions, output saturation level, and anti-windup configuration. In this work, we will use the current configuration of the controller, i.e. a PID controller in parallel form with a discrete time domain without anti-windup. Once the operating point of the SEPIC converter has been determined, the next step is to identify the system parameters. For identification, a finite value for the Simulink model's stopping time must be specified. Then the input data of the I/O will be used as the input of the Simulink identification system. The simulation of the system as seen by the controller has started. The software temporarily removes the PID Controller block from the model, then injects a signal at the location of the PID block output and measures the resulting signal at the location of the PID block input. This data describes the system response as seen by the controller. Based on this response, a linear model of the SEPIC converter is estimated. The excitation signal is a step whose properties are given in Figure 6

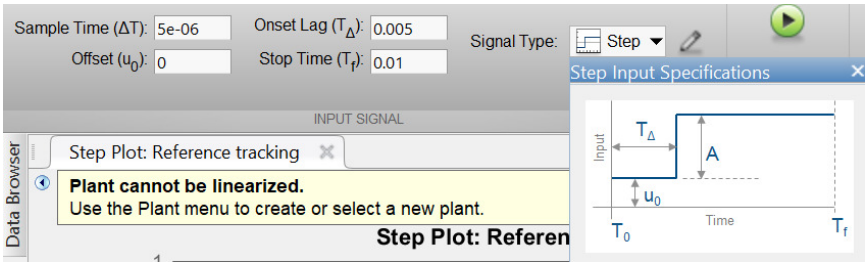

Figure 6: excitation signal Input Specifications

SIMULINK's PID Tuner utility identifies the equivalent model using the data generated by the open-loop model simulation. The model parameters are set so that the identified system response, when receiving the measured input, matches the measured output.

Estimation Progress

```
Estimating measured dynamics model...
Algorithm: Nonlinear least squares with automatically chosen line search method
-------------------------------------------------------------------------------------
                          Norm of     First-order     Improvement (%)
Iteration      Cost       step        optimality    Expected  Achieved   Bisections
-------------------------------------------------------------------------------------
    0       11.7763         -           23.4        7.22         -          -
    1       2.14033   1.01e+03           143        7.22        81.8        1
    2      0.811252        329           315        45.4        62.1        0
    3     0.0264354         53           283         119        96.7        0
    4     0.0258499      0.158        0.0132        83.8        2.21        0
    5     0.0258499    0.00206      2.91e-05    1.48e-05    3.87e-07        0
    6     0.0258499   3.28e-05      4.63e-07    3.69e-09    4.03e-11        0
-------------------------------------------------------------------------------------
```

Result

```
Termination condition: Near (local) minimum, (norm(g) < tol)..
Number of iterations: 6, Number of function evaluations: 14

Status: Estimated using PEM with prediction focus
Fit to estimation data: 97.61%, FPE: 0.0259534
```

Figure 7:SEPIC model estimation progress and results

After system identification, we found that the Prediction error estimate for linear and nonlinear model usingprediction estimation method (PEM) was able to generate a model that made the real system within 97.61% as shown in Fig. 7. The approximation model adopted is a first-order system whose transfer function is given by equation (3).

$$TF = \frac{K_s}{1 + \tau . p} \tag{3}$$

After identifying the transfer function of the SEPIC converter to a selected operating point in steady state, this function will be used to determine the parameters of the controller. An identification algorithm will be executed based on the selected input performance to produce the optimal combination of the three controller actions. The result of the controller parameters as well as the performance and robustness indications are shown in F Figure 8: PID controller parameters and response performance

Controller Parameters

	Tuned	Block
P	0.018901	0.018901
I	27.7028	27.7028
D	n/a	n/a
N	n/a	n/a

Performance and Robustness

	Tuned	Block
Rise time	0.0013 seconds	0.0013 seconds
Settling time	0.00459 seconds	0.00459 seconds
Overshoot	7.76 %	7.76 %
Peak	1.08	1.08
Gain margin	Inf dB @ NaN rad/s	Inf dB @ NaN rad/s
Phase margin	70 deg @ 1.2e+03 ra...	70 deg @ 1.2e+03 ra...
Closed-loop stability	Stable	Stable

Figure 8: PID controller parameters and response performance

Microcontroller implementation

1.6 PIC18F4550 Microcontroller

For the PID controller implementation, we opted for the PIC18F microcontroller from Microchip Technology. This range of microcontrollers has an 8-bit processor and offers more performance compared to the PIC16F family. The PIC18Fxxxx microcontroller family can operate at speeds up to 12 MIPS (12 Million Instructions per Second) and has a hardware accelerator to optimize execution time and increase CPU performance[19]. Among the hardware accelerator that have completely changed the structure of this family

is the hardware multiplier. The latter is widely used for faster control algorithms calculation, which is an asset for our application due to the large number of operations that can be contained in the intended applications. Matrix calculation in the PID algorithm, for example. The PIC18F4550 therefore has higher computing power and allows a code size reduction for multiplication algorithms. In addition, it can handle many applications that were previously reserved for digital signal processors (DSP). A comparison of various hardware and software multiplication operations, as well as the savings in memory and execution time, is shown in TABLE III.

TABLE III HARDWARE VS SOFTWARE MULTIPLY TIMING

Routine	Multiply Method	Program Memory (Words)	Cycles (Max)	Time		
				@ 40 MHz	@ 10 MHz	@ 4 MHz
8 x 8 unsigned	Without hardware multiply	13	69	6.9 µs	27.6 µs	69 µs
	Hardware multiply	1	1	100 ns	400 ns	1 µs
8 x 8 signed	Without hardware multiply	33	91	9.1 µs	36.4 µs	91 µs
	Hardware multiply	6	6	600 ns	2.4 µs	6 µs
16 x 16 unsigned	Without hardware multiply	21	242	24.2 µs	96.8 µs	242 µs
	Hardware multiply	28	28	2.8 µs	11.2 µs	28 µs
16 x 16 signed	Without hardware multiply	52	254	25.4 µs	102.6 µs	254 µs
	Hardware multiply	35	40	4.0 µs	16.0 µs	40 µs

In addition, there are variants in the PIC18F family with specialized control peripherals, including a PWM hardware module capable of generating pulse-width modulated signals, which is widely used in many applications. In our study, the PIC18F4550 was used to generate PWM signals. It is capable of generating a very high PWM frequency. It has two RC1 and RC2 channels to produce PWM. The CCP module has several operating modes, but in this work, it will be used in the PWM one. To force this mode, the first three bits of the ECCPxCON control register must be set and the proper configuration must be done. The PWM of a specific frequency is created by setting the proper clock value to force the desired PWM period. The required clock value is determined by the following equation (4).

$$PWM\ Period = [(PR2) + 1] \times 4 \times T_{OSC} \times (TMR2\ Prescale) \quad (4)$$

In this work, the microcontroller is synchronized using a 20 MHz crystal oscillator. By choosing a suitable value in the PR2 register and the TMR2 prescale, we can specify the period of the PWM control signal and, therefore, the operating frequency (39 KHz is selected for the hardware during the test). Other variants of the PIC18F family have an ECCP module, which is also found on the peripherals of the PIC16Fxx family. It is capable of synchronizing the control and digital acquisition of multi-input systems. The source code developed for the PIC16F family can be easily migrated to this controller family. In addition, it has a complete analog acquisition interface with TTL electrical levels (0-5V) with the possibility to choose other references, including negative ones. The PIC18f4550 offers the advantages of all PIC18 microcontrollers' series; high performance at an economical price, enhanced high performance flash memory, hardware accelerators and serial communication modules such as USB. In addition to these features, the PIC18F4550 family introduces design enhancements that make these microcontrollers a logical choice for many applications that require high runtime performance and low power consumption, which is exactly the need of our real-time embedded solution.

1.7 Hardware implementation

After designing, sizing, and simulating our SEPIC converter, and the control structure under the MATLAB/Simulink environment, we proceed directly to the practical part of this work, which is divided into two elementary phases. The first one is the choice of the components to realize the SEPIC system, and for that, we have to respect several constraints imposed by the component availability in the market. As a power switch, a power transistor of the IRF230 MOSFET type will be used. In contrast to the transistor control in the MATLAB/Simulink simulations, this element cannot be driven directly by a logic circuit, so an electrical level adaptation stage called a driver must be used. It must be inserted between the transistor and the control unit. As a driver, we have chosen the IR2112 component. To recover the output voltage, we use a voltage sensor in the form of a voltage divider dimensioned to be able to measure the maximum voltage that the SEPIC converter can produce. An alphanumeric LCD display is also used in the assembly to display system related information such as the set point and the actual output voltage.

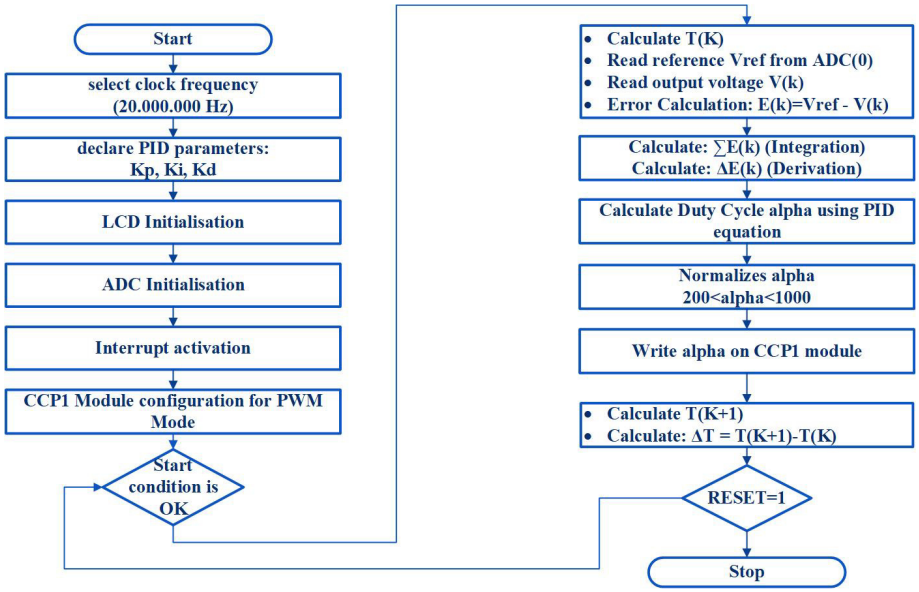

Figure 9: PID implementation algorithm on PIC18F4550

As far as the control part is concerned, as mentioned above, the PID control algorithm will be implemented in the PIC18F4550 microcontroller. In addition to developing the control law, this processing unit transforms the control signal $U(t)$ into a real PWM control signal that will directly drive the transistor. In addition, the microcontroller manages at the same time the display of the information on the LCD display. Three potentiometers, RV1, RV2 and RV3, are connected to the analog port of the MCU, which reads and analyzes in real time the analog values on the port and transforms them into a suitable range to adjust the gains rates of the PID regulator. The complete electronic circuit is given in Figure 10.

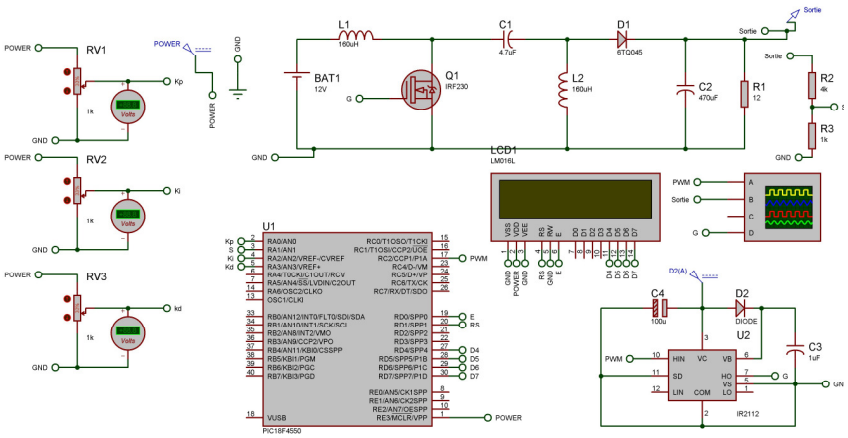

Figure 10: Electronic schematic of SEPIC controlled PID system

Results and Discussion

After designing the SEPIC converter, and following the process of implementing a PID controller to improve the performance of this system, whether in terms of dynamics, accuracy, or stability, we now move to the validation phase and results analysis. To do so, this part will be divided into two phases. First, we will discuss the results obtained under the MATLAB/Simulink environment, then move on to the actual validation stage under the PROTEUS simulation environment. As mentioned previously, the objective of this work is to develop a power converter capable of generating from a fixed or variable voltage a well-regulated voltage output. This voltage must be between 0 and 24 volts, which is the possible set point range for this system. The SEPIC system tested is the one given in Fig. 5 with an input voltage equal to 12 volts. The verification of the system behavior following several set points will be done. The chosen test values coincide perfectly with the values of the standard power supplies or voltage sources. Fig. 11 shows the response of the system to 5, 9, 12, 15, 18 and 24 volts respectively. It can be clearly seen that the system is capable of precisely following the required set points, guaranteeing high performance with a response time of no more than six milliseconds in the case of a 24-volt set point. In addition, it is clearly noticeable that the system is perfectly stable and that the errors are negligible.

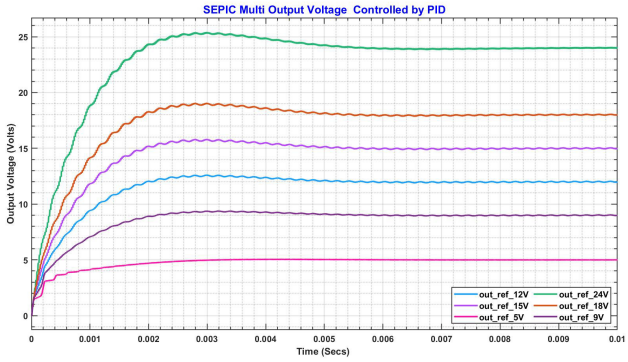

Figure 11: SEPIC multi output voltage controlled by PID (VIN = 12 volts)

After verifying the correct behavior of the SEPIC converter in terms of reference tracking, the second test consists of checking the system robustness following a load variation for the same reference. **Erreur ! Source du renvoi introuvable.**12shows the system response for several load values, respectively 20, 50, 100, and 10 Ohms. It can be

noticed that the transient behavior becomes worse as the load increases, and the system behaves like a second order and presents oscillations, but the proposed controller is able to drive the response towards the desired value while still guaranteeing the selected performance. The response time does not exceed 20 Milliseconds for a 100 Ohms load. Stability is always guaranteed and accuracy is acceptable.

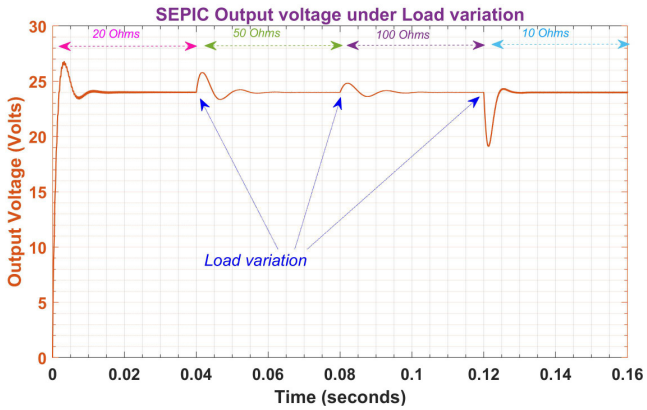

Figure 12: SEPIC Output voltage under Load variation (VIN = 12 volts)

The test scenario that follows is a mixture between a reference change and a load variation in the same simulation cycle. The process is as follows: at the beginning, a set point of 18 volts and a constant load are chosen, then at the 50 millisecond instant, the set point is abruptly changed from 18 to 5 volts, and at the instant of 75 milliseconds, the load is changed and the reference is kept at 5 volts. The response of the designed system to this test is given in Fig. 13. It can be noticed that the system always keeps its performance and resists to the reference change and load perturbation.

The final verification test is performed to check the system's performance against one or more disturbances from the source, which is no longer constant in this case. For this purpose, we will set the set point at 18 volts, and at the input, we will choose a multi-level voltage source. The expected result of this test is to have an output equal to the value of the selected set point and the system rejects more quickly the disturbances produced due to the input voltage change of the converter system. The predictable behavior of this test is confirmed by the result shown in Fig. 14. In this test, we have considered three levels of input voltage, respectively, 12, 9 and 15 volts; the load value is fixed at 10 Ohms. The system shows again that it is able to reject any source of disturbance and guarantee an optimal response. The selected set point is 18 volts.

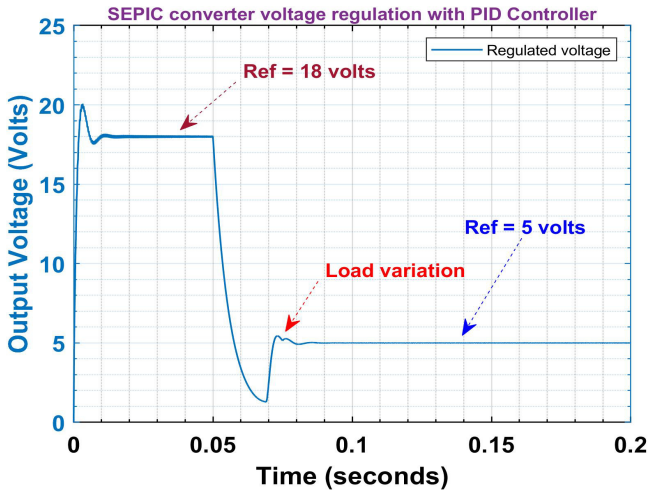

Figure 13: Load and reference variation test (VIN = 12 volts)

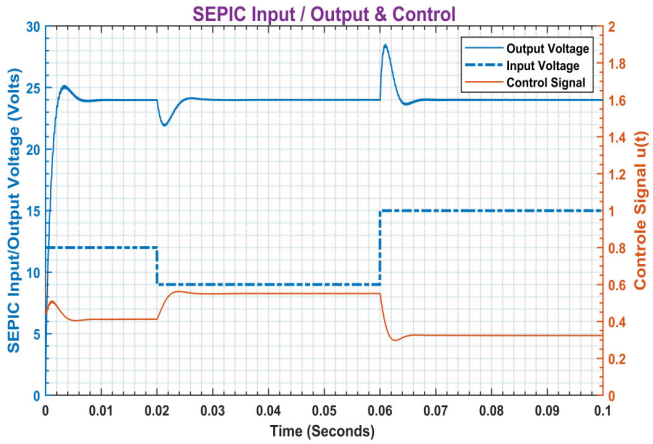

Figure 14: SEPIC Input voltage perturbation test

The control law produced by the controller that gives the results is given in Fig. 14 (orange signal). We can clearly notice the ability of the controller to reject each time the disturbances that appears in the system. Now, after having validated the correct operation of our design to regulate the SEPIC converter output voltage, we move on to practical PID algorithm validation in hardware. The PID regulator is fully implemented on the PIC18F4550 microcontroller. The results given by Fig. 15 and Fig. 16 show clearly the correct operation of our system on the hardware target. The two output voltage responses are tested respectively at 24 volts and 15 volts. The microcontroller is therefore running the PID algorithm in such a way to achieve the same performance confirmed by MATLAB/Simulink simulation.

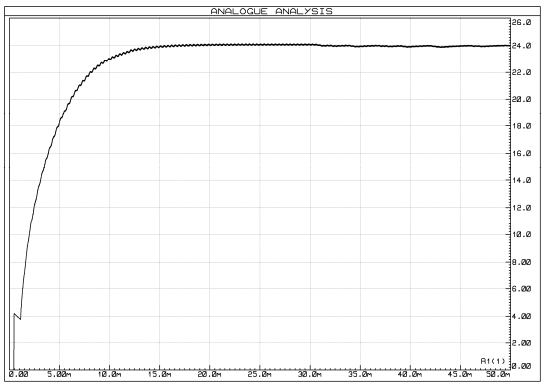

Figure 15: SEPIC voltage output controlled by PIC18F4550 (REF = 24V)

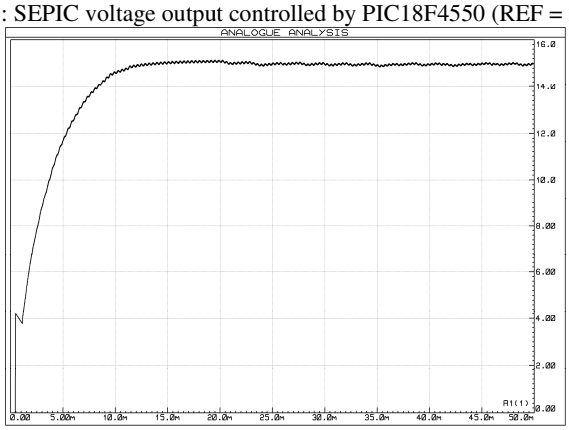

Figure 16: SEPIC voltage output controlled by PIC18F4550 (REF = 15V)

Figure 17shows the hardware information of our microcontroller implementation, including the used reference, the XC8 compiler, the memory space consumed on the flash program memory as well as the reserved space on the RAM, and the debugging andprogramming tool PICkit3

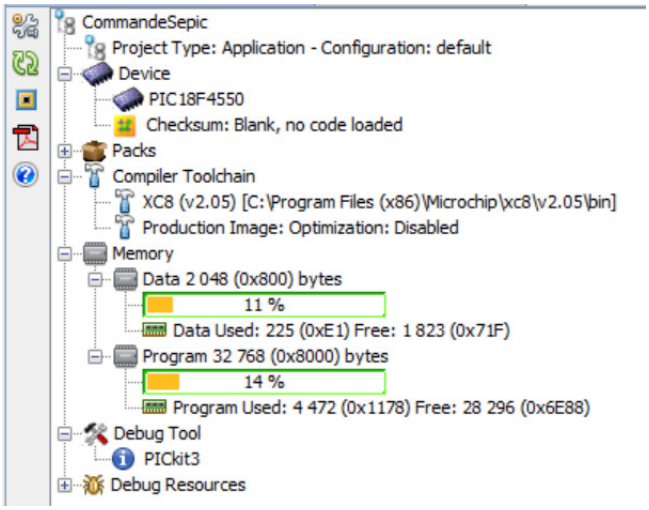

Figure 17: Hardware implementation information

Conclusion

In this work, we have developed a DC/DC conversion system including a PID controller. The objective is to optimize and implement a digital controller version to regulate the output voltage. The embedded target selected for this work is the low-cost 8-bit microcontroller. We started by sizing and simulating the open-loop system, then we linearized the model at an operating point to derive the equivalent transfer function of the system, then we inserted the regulator whose parameters were identified based on the estimated linear model of the converter. The set of simulations performed under MATLAB/Simulink show the good performance of our solution. The performed simulations and test scenarios clearly demonstrate the system dynamics, which became fast, as well as the stability and accuracy of the response. After all simulations, a migration to hardware was done by implementing the PID controller on a PIC18F4550 microcontroller. The implementation results proved that the entire SEPIC/PID system worked well experimentally based on real models of the electronic components in the PROTEUS environment. This solution may be used in a wide range of applications, such as MPPT solar regulators and battery management systems (BMS). In terms of economics, this system has a good performance to price ratio since we were able to implement advanced functionalities in a low-cost 8-bit microcontroller. Consequently, as a perspective of this paper, we aim to apply all the proposed solutions in this work to develop a BMS battery management system for photovoltaic applications.

References

[1] P. Swain, S. Jagadish, and K. N. S. U. Mahesh, "Integration of renewable sources of energy into power grid," *TENSYMP 2017 - IEEE Int. Symp. Technol. Smart Cities*, Oct. 2017, doi: 10.1109/TENCONSPRING.2017.8070012.

[2] B. S. Pali and S. Vadhera, "Renewable energy systems for generating electric power: A review," *1st IEEE Int. Conf. Power Electron. Intell. Control Energy Syst. ICPEICES 2016*, Feb. 2017, doi: 10.1109/ICPEICES.2016.7853703.

[3] R. W. De Doncker, C. Meyer, R. U. Lenke, and F. Mura, "Power electronics for future utility applications," *Proc. Int. Conf. Power Electron. Drive Syst.*, 2007, doi: 10.1109/PEDS.2007.4487666.

[4] Z. Sabiri, N. Machkour, E. Kheddioui, M. B. Camara, and B. Dakyo, "DC/DC converters for photovoltaic applications-modeling and simulations," *Proc. 2014 Int. Renew. Sustain. Energy Conf. IRSEC 2014*, pp. 209–213, Mar. 2014, doi: 10.1109/IRSEC.2014.7059812.

[5] A. Gaga, O. Diouri, N. Es-Sbai, and F. Errahimi, "Design and realization of an autonomous solar system," *IOP Conf. Ser. Mater. Sci. Eng.*, vol. 186, no. 1, Mar. 2017, doi: 10.1088/1757-899X/186/1/012031.

[6] M. M. U. Rehman, F. Zhang, R. Zane, and D. Maksimovic, "Design and control of an integrated BMS/DC-DC system for electric vehicles," *2016 IEEE 17th Work. Control Model. Power Electron. COMPEL 2016*, Aug. 2016, doi: 10.1109/COMPEL.2016.7556729.

[7] A. Bubovich, "The comparison of different types of DC-DC converters in terms of low-voltage implementation," *Proc. 5th IEEE Work. Adv. Information, Electron. Electr. Eng. AIEEE 2017*, vol. 2018-January, pp. 1–4, Jul. 2017, doi: 10.1109/AIEEE.2017.8270560.

[8] O. Diouri, N. Es-Sbai, F. Errahimi, A. Gaga, and C. Alaoui, "Control of single phase inverter using back-stepping in stand-alone mode," *2019 Int. Conf. Wirel. Technol. Embed. Intell. Syst. WITS 2019*, Apr. 2019, doi: 10.1109/WITS.2019.8723761.

[9] A. C. C. Hua and B. C. H. Cheng, "Design and implementation of power converters for wind energy conversion system," *2010 Int. Power Electron. Conf. - ECCE Asia -, IPEC 2010*, pp. 323–328, 2010, doi: 10.1109/IPEC.2010.5542251.

[10] O. Diouri, A. Gaga, N. Es-Sbai, and F. Errahimi, "Design and simulation of a novel cascaded transformer multilevel inverter topology for photovoltaic system," *Proc. 2015 IEEE Int. Renew. Sustain. Energy Conf. IRSEC 2015*, Apr. 2016, doi: 10.1109/IRSEC.2015.7454957.

[11] F. A. Samman and A. Azhari, "DC/AC power converter for home scale electricity systems powered by renewable energy," *2016 Int. Conf. Smart Green Technol. Electr. Inf. Syst. Adv. Smart Green Technol. to Build Smart Soc. ICSGTEIS 2016 - Proc.*, pp. 149–154, Mar. 2017, doi: 10.1109/ICSGTEIS.2016.7885782.

[12] P. P. Surya, D. Irawan, and M. Zuhri, "Review and comparison of DC-DC converters for maximum power point tracking system in standalone photovoltaic (PV) module," *Proceeding - ICAMIMIA 2017 Int. Conf. Adv. Mechatronics, Intell. Manuf. Ind. Autom.*, pp. 242–247, Jun. 2018, doi: 10.1109/ICAMIMIA.2017.8387595.

[13] J. C. Mayo-Maldonado, O. F. Ruiz-Martinez, G. Escobar, J. E. Valdez-Resendiz, T. M. Maupong, and J. C. Rosas-Caro, "Nonlinear Stabilizing Control Design for DC-DC Converters Using Lifted Models," *IEEE Trans. Ind. Electron.*, vol. 68, no. 11, pp. 10772–10783, Nov. 2021, doi: 10.1109/TIE.2020.3031530.

[14] S. Mouslim, M. Oubella, M. Kourchi, and M. Ajaamoum, "Simulation and analyses of SEPIC converter using linear PID and fuzzy logic controller," *Mater. Today Proc.*, vol. 27, pp. 3199–3208, Jan. 2020, doi: 10.1016/J.MATPR.2020.04.506.

[15] R. P. Aguilera, P. Acuna, G. Konstantinou, S. Vazquez, and J. I. Leon, "Basic Control Principles in Power Electronics: Analog and Digital Control Design," *Control Power Electron. Convert. Syst.*, pp. 31–68, Jan. 2018, doi: 10.1016/B978-0-12-805245-7.00002-0.

[16] T. Haripriya, A. M. Parimi, and U. M. Rao, "Modeling of DC-DC boost converter using fuzzy logic controller for solar energy system applications," *Asia Pacific Conf. Postgrad. Res. Microelectron. Electron.*, pp. 147–152, 2013, doi: 10.1109/PRIMEASIA.2013.6731195.

[17] P. K. Maroti, S. Padmanaban, J. B. Holm-Nielsen, M. Sagar Bhaskar, M. Meraj, and A. Iqbal, "A New Structure of High Voltage Gain SEPIC Converter for Renewable Energy Applications," *IEEE Access*, vol. 7, pp. 89857–89868, 2019, doi: 10.1109/ACCESS.2019.2925564.

[18] Y. Zhang, Y. Jia, T. Chai, D. Wang, W. Dai, and J. Fu, "Data-Driven PID Controller and Its Application to Pulp Neutralization Process," *IEEE Trans. Control Syst. Technol.*, vol. 26, no. 3, pp. 828–841, May 2018, doi: 10.1109/TCST.2017.2695981.

[19] A. Gaga, Y. Mehdaoui, S. El Ouahdani, B. El Hadadi, and F. Errahimi, "Embedded Hardware/Software CAN Node Design for Engineering and Research in the Automotive Application Field," *Int. J. Eng. Appl.*, vol. 10, no. 2, p. 126, Mar. 2022, doi: 10.15866/IREA.V10I2.20813.